Journal of Materials Science: Materials in Electronics (2018) 29:3104–3109
https://doi.org/10.1007/s10854-017-8242-2

Effect of co-doping Y_2O_3–La_2O_3 on microstructure and electrical properties of ZnO-based varistor ceramics prepared from nanosize ZnO powder

Shuaijun Yang[1] · **Dachuan Zhu**[1]

Received: 1 September 2017 / Accepted: 9 November 2017 / Published online: 14 November 2017

Abstract

ZnO-based varistor ceramics doped with fixed La_2O_3 and different Y_2O_3 have been fabricated by the conventional solid-state reaction route. Phase composition, microstructure, and electrical properties were studied by X-ray diffractometry (XRD), scanning electron microscopy (SEM), and direct current electrical measurement. The Y_2O_3 phase, Y-rich phase and La-rich phase were found to distribute along the grain boundaries of predominant ZnO grains from XRD and SEM analyses. The average grain size of the primary phases was calculated to be in the range of 3.80 to 4.17 µm. The varistor ceramic doped with 0.1 mol% La_2O_3 and 0.5 mol% Y_2O_3 sintered at 1100 °C for 2 h exhibited high comprehensive electrical properties with the breakdown field of 1055 V/mm, the nonlinear coefficient of 65.5 and the leakage current of 0.6 µA. The results illustrated that co-doping La_2O_3 and Y_2O_3 and employing the ZnO powder in nanometer size may be a promising route to obtain varistor ceramics with excellent electrical properties.

1 Introduction

ZnO varistor ceramics have been widely applied in overvoltage protection and voltage stabilization owing to their large-surge-handling capability and highly nonlinear volt-ampere characteristics enabling them functionally equivalent to a reversible, solid-state switch [1–3]. In normal operative mode, ZnO varistors are subject to a voltage below their switch voltage, meanwhile a small leakage current flows through the varistors. When the applied voltage exceeds the switch voltage on occasion, ZnO varistor act as a conductor and surges pass. Moreover, when the voltage returns to the normal state, the varistors are able to recover to high resistive state.

ZnO varistor ceramics conventionally are fabricated via sintering pressed shapes of mixtures of ZnO powder with small quantity of additives, such as Bi_2O_3, Sb_2O_3, Cr_2O_3, Co_2O_3, MnO_2 etc [3, 4]. In the process of sintering and cooling, a thin insulating layer forms by segregation of above mentioned dopants along the semiconducting n-type ZnO grain boundaries, which induces the double Schottky barrier and consequently brings the nonlinear volt-ampere properties [5]. The breakdown field of ZnO varistors closely relating to the height of Schottky barrier and the nonlinear coefficient α of nonlinear volt-ampere properties are critical parameters for the varistor function, both determing the capability of protection for electronic components or circuits [6, 7].

As is well-known, doping of rare earth elements can affect the microstructure transformation of ZnO and control the grain size of ZnO effectively [8]. Although the studies of ZnO varistor ceramics have been conducted for many years, the hot spots and focus of the investigation of ZnO varistors recently turn to the application of nanometer powder in ZnO varistors and the effect of different rare earth oxides, such as yttrium oxide, lanthanum oxide, europium oxide, on microstructure and electrical properties [9–12]. Bernik et al. [13] reported that a fine-grained and uniformly distributed Y_2O_3-containing phase was a very effective grain-growth inhibitor, which directly results in the augment of breakdown field (threshold voltage). Houabes et al. [12] found that addition of La_2O_3 increased the breakdown field of $ZnO–Bi_2O_3$-based ZnO varistor ceramics. Xu et al. [14] reported the effect of La_2O_3 on microstructure and electrical properties of ZnO-based varistor ceramics; their results

---

✉ Dachuan Zhu
zhudachuan@scu.edu.cn

[1] College of Material Science and Engineering, Sichuan University, Chengdu 610065, Sichuan, People’s Republic of China

showed that ZnO-based varistor ceramics with addition of 0.08 mol% La_2O_3 exhibited comparatively ideal comprehensive electrical properties with E_b of 320V/mm, α of 36.8 and I_L of 0.29 μA. Tu et al. [15] reported that Y_2O_3 additives reacted with other dopants and generated new phases which caused the grain to decrease and grain boundary area to increase. Thus, fine-grained varistor ceramics are demanded for high voltage application and electrical properties of varistor ceramics can be modified by the addition of several dopants. The detailed performance parameters of these parallel works carried out are presented in Table 1.

In order to obtain high electrical performance, La_2O_3 and Y_2O_3 are added to ZnO–Bi_2O_3-based varistor ceramics in this work. Furthermore, the Zinc Oxide is employed in nanometer size. The effect of incorporation of La_2O_3 and Y_2O_3 on the microstructure and electrical characteristics of ZnO–Bi_2O_3-based varistors prepared from nanosize ZnO powder was investigated.

2 Experimental

ZnO–Bi_2O_3-based varistor ceramics were prepared by the conventional solid-state reaction route. Analytical-grades raw materials with a nominal composition of (96.7 − x) mol% ZnO, 0.7 mol% Bi_2O_3, 1.0 mol% Sb_2O_3, 0.5 mol% Cr_2O_3, 0.5 mol% Co_2O_3, 0.5 mol% MnO_2, 0.1 mol% La_2O_3 and x mol% Y_2O_3 (x = 0.0, 0.1, 0.3, 0.5, 0.7, 0.9) were mixed by ball-milling with agate balls and anhydrous alcohol in agate jars for 24 h and then dried at 60 °C for 12 h followed by calcination at 400 °C for 1 h. Next, the mixture of powders was added with approximately 5 wt% polyvinyl alcohol solution and pressed uniaxially into disks with diameter of 15 mm and thickness approximately of 1.3 mm at a pressure of 100 Mpa. The pressed disks were sintered at 1100 °C for 2 h in air, followed by furnace cooling. Both surfaces of sintered disks were polished and coated with sliver paste to form electrodes by heating at 870 °C for 1 h.

To expose the microstructure for observation, the disks were ground with silicon carbide paper and polished with chromium trioxide powder. Then, the polished samples were cleaned ultrasonically with alcohol for 40 min to remove adhering particles. Finally, the polished ceramics were thermally etched at 1000 °C for 20 min in air.

The crystalline phases were identified by use of a DX-1000 diffractometer with CuKα radiation operating at 40 kV/25 mA. The morphology of the ceramics was characterized through a scanning electron microscope (SEM, JSM-7500F; Jeol, Japan) equipped with energy-dispersive X-ray spectroscopy (EDS).

The average grain size, D, was calculated by the linear intercept method via the equation:

$$D = 1.56L/MN \tag{1}$$

where L is a random straight line length on the micrograph, M the magnification of the micrograph, and N the number of grain boundaries intercepted by the lines. Direct current (DC) electrical measurements at room temperature were carried out on an MY-3 kV meter. The nominal varistor voltage, V_{1mA}, was detected at 1 mA and the breakdown field, E_b (V/mm), was calculated via the equation $E_b = V_{1mA}/H$, where H is the thickness of the sample in mm. The leakage current I_L was measured at a voltage of $0.75V_{1mA}$. The nonlinear coefficient α was calculated via the equation:

$$\alpha = 1/\lg(V_{1mA}/V_{0.1mA}) \tag{2}$$

where V_{1mA} and $V_{0.1mA}$ are the electric voltages at currents of 1 and 0.1 mA, respectively.

3 Result and discussion

XRD patterns of the investigated samples are presented in Fig. 1. The ZnO primary phase, spinel phase, Bi_2O_3-rich phase, La-rich phase, Y_2O_3 phase and Y-rich phase are identified. Additional peaks are observed in samples doped with Y_2O_3 due to formation of a Y-rich phase and Y_2O_3 phase in the varistor ceramics. At the same time, some of the peaks corresponding to spinel phase of $Zn_7Sb_2O_{12}$ diminish with higher content of Y_2O_3.

Figures 2 and 3 respectively show the SEM micrographs of ZnO-based varistor ceramics with different Y_2O_3 contents and representative results from EDS analysis of ZnO–Bi_2O_3-based varistor ceramics containing 0.5 mol% Y_2O_3.

Table 1 Various ZnO varistors with different composition surveyed in literatures

Material composition	E_b (V/mm)	α	I_L (μA)	References
ZnO–Bi_2O_3–Sb_2O_3–Co_3O_4–Cr_2O_3–MnO_2–NiO–Sm_2O_3	197–322	20–58	1.1–12.0	[8]
ZnO–Bi_2O_3–Sb_2O_3–Co_3O_4–Cr_2O_3–Mn_3O_4–NiO–Y_2O_3	166–217	–/–[a]	0.1–2.2	[13]
ZnO–Bi_2O_3–Sb_2O_3–Co_3O_4–Cr_2O_3–MnO_2–NiO–B_2O_3–MgO–Al_2O_3–La_2O_3	220–290	–/–	–/–	[12]
ZnO–Bi_2O_3–Sb_2O_3–Co_2O_3–Cr_2O_3–MnO_2–La_2O_3	77–503	2.4–36.8	0.09–494	[14]
ZnO–Bi_2O_3–Sb_2O_3–Co_2O_3–Cr_2O_3–MnO_2–$Ag(NO_3)_3$–SiO_2–Y_2O_3	255–367	6.6–18.4	34–129	[15]

[a] Means the corresponding information is not mentioned in the original document

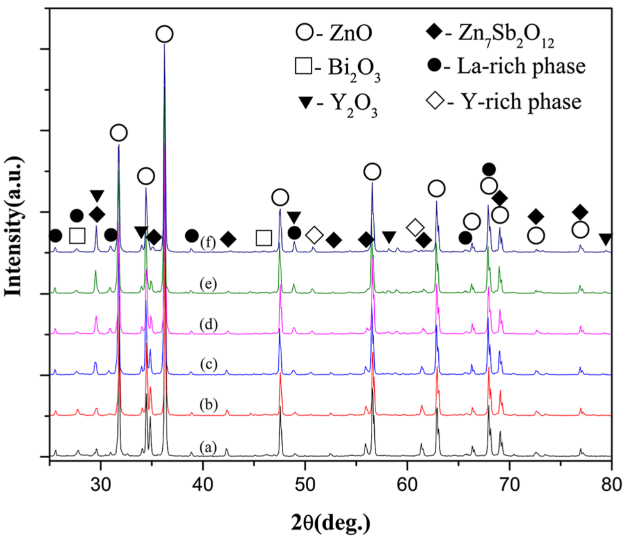

Fig. 1 XRD patterns of the varistor ceramics doped with different amounts of Y_2O_3 sintered at 1100 °C for 2 h: **a** 0.0 mol%, **b** 0.1 mol%, **c** 0.3 mol%, **d** 0.5 mol%, **e** 0.7 mol%, **f** 0.9 mol%

The SEM micrographs reveal that ZnO grains are surrounded by many minor secondary phases along the grain boudary. The element constitution identified by EDS analysis confirms the existence of phases of the samples already determined by the XRD analysis.

As shown in the EDS analysis, the secondary phase has different composition from the ZnO phase; the presence of Y-rich phase can be found. No La peak is found within the EDS detection limit.

As shown in Fig. 4, the average grain size of ZnO varistors is calculated by the linear interception method to be 4.17, 3.99, 3.82, 3.80, 3.88 and 3.91 μm corresponding to the rising Y_2O_3 content of 0.0, 0.1, 0.3, 0.5, 0.7, and 0.9 mol%, respectively. That the average grain size of ZnO varistors initially decreases and then increases can be explained as follows.

As the La^{3+} ions (0.106 nm) and Y^{3+} ions (0.089 nm) have larger radius than Zn^{2+} (0.074 nm), the solid solubility of the La^{3+} and Y^{3+} ions into ZnO grains is very low, La^{3+} ions and Y^{3+} ions are mainly distributed on the grain boundaries in which La^{3+} ions form La-rich phases and Y^{3+} ions form Y-rich phases or Y_2O_3 oxide alone in agreement with the results of Ke et al. [16]. These phases may inhibit ZnO grain growth by a pinning effect [2]. And, with the Y_2O_3 content increasing, more Bi_2O_3 rich liquid phase which should promote mobility of grain boundaries is depleted by reacting with Y_2O_3. Therefore, the average size of ZnO grains is diminished.

On the other hand, it also can be noticed from XRD patterns that the amount of the $Zn_7Sb_2O_{12}$ phase decreases with increasing Y_2O_3 content, resulting in the increase of ZnO grain size as it also acts as a moderator of the growth of ZnO grains, in agreement with the report by Xu et al. [17].

With the interaction of above two contrary effects, the average grain size of ZnO varistors initially ascends and then descends.

The electrical properties including breakdown field E_b, leakage current I_L and nonlinear coefficient α of the ZnO–Bi_2O_3 varistors ceramic are measured. As can be seen from the Fig. 4, doped Y_2O_3 visibly influences the breakdown field of varistors. With the increasing content of Y_2O_3, the breakdown field of the ceramic regularly initially ascends from 795 to 1055 V/mm and then descends to 960 V/mm. The maximum E_b of 1055 V/mm, which highly surpasses the values of the La_2O_3-doped Varistors or other parallel works, corresponds to the minimum value of D [12–15]. According to the Schottky barrier model, which is mainstream theory used for clarifying the nonlinear characteristic of ZnO varistors, $E_b = nU_{gb}$, where n is the number of grain boundaries per unit length and U_{gb} is the voltage drop per grain boundary. The variation of the breakdown field hence goes against the variation of the average size of ZnO grains. Consequently, the smaller grain size, D, of varistor ceramics results in the higher value of n, and in turn increases the breakdown voltage, as reported by Ramírez et al. [18].

Figure 5 shows the variation of α and I_L with molar concentration of Y_2O_3 in ZnO–Bi_2O_3-based varistor ceramics sintered at 1100 °C for 2 h. It is observed that the nonlinear coefficient, α, initially increases from 50.3 to 65.5 and then decreases to 52.6. The maximum value of α (65.5) is much higher than that of the La_2O_3 doped varistors (< 40) and slightly higher than that of the Sm_2O_3 doped varistors (58) [8, 14].

It was reported that although the radius of Y^{3+} is slightly larger than that of Zn^{2+}, limited substitution within the ZnO grains is promoted for a high sintering temperature of 1100 °C facilitates the solid solution reaction [16]. Meanwhile, positron centers and valence electrons will be produced. Therefore, the doped Y_2O_3 is involved in the formation of lattice defects and deep bulk traps, both of which enhance nonlinear performance [19]. And as more content of Y_2O_3 is doped, the more lattice defects and deep bulk traps emerge. Consequently, the nonlinear coefficient α gradually increases with the amounts of Y_2O_3 increasing from 0 to 0.5 mol%. However, as the Y_2O_3 content continues to increase from 0.5 to 0.9 mol%, a growing number of Y_2O_3 additives exist in grain boundaries to react with other dopants, generating new phases and decreasing the donor ions segregated at the depletion layer. These actions in turn cause the defects in ZnO varistors to decrease. As a result, the donor density and interface state density (N_S) decrease with the Y_2O_3 content increasing. According to the formula:

$$\phi_B \propto N_S^2 \tag{3}$$

and the higher Schottky barrier at the grain boundary contributes to a larger nonlinear coefficient α. Thus, the

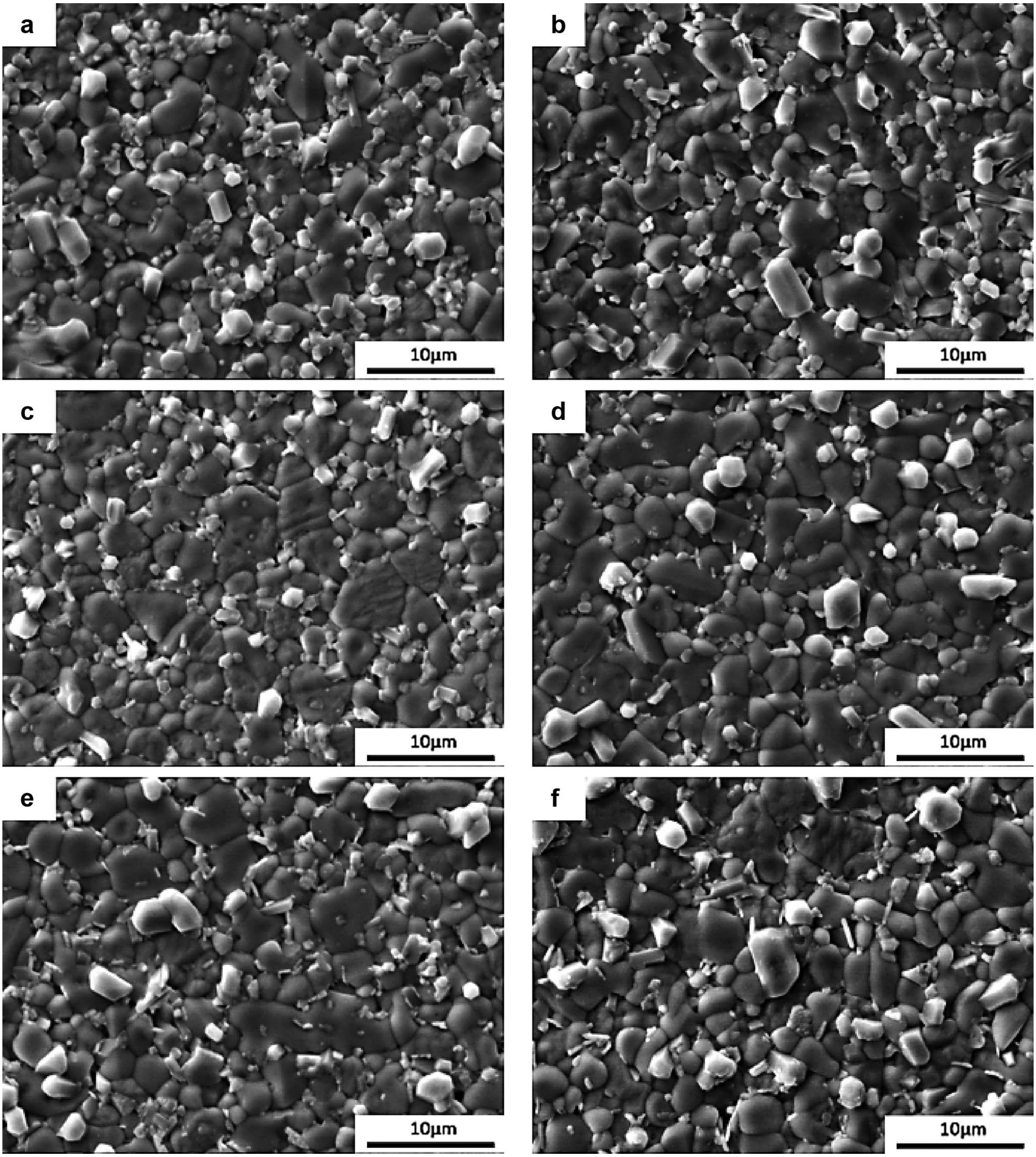

Fig. 2 SEM micrographs of the varistor ceramics doped with different amounts of Y_2O_3 sintered at 1100 °C for 2 h: **a** 0.0 mol%, **b** 0.1 mol%, **c** 0.3 mol%, **d** 0.5 mol%, **e** 0.7 mol%, **f** 0.9 mol%

nonlinear coefficient α decreases when the Y_2O_3 content increases from 0.5 to 0.9 mol%.

The leakage current, I_L, gradually increases from 0.2 to 1.0 μA with Y_2O_3 content increasing. The values of I_L are lower than that of the La_2O_3 and Sm_2O_3 co-doped varistors and more stable than that of the La_2O_3 doped varistors [14, 20]. The variation can be attributed to that as Y_2O_3 content increases more Y-rich phases forms at the grain boundaries of ZnO, and these phases influences the distribution of all other varistor dopants along the grain boundaries of ZnO.

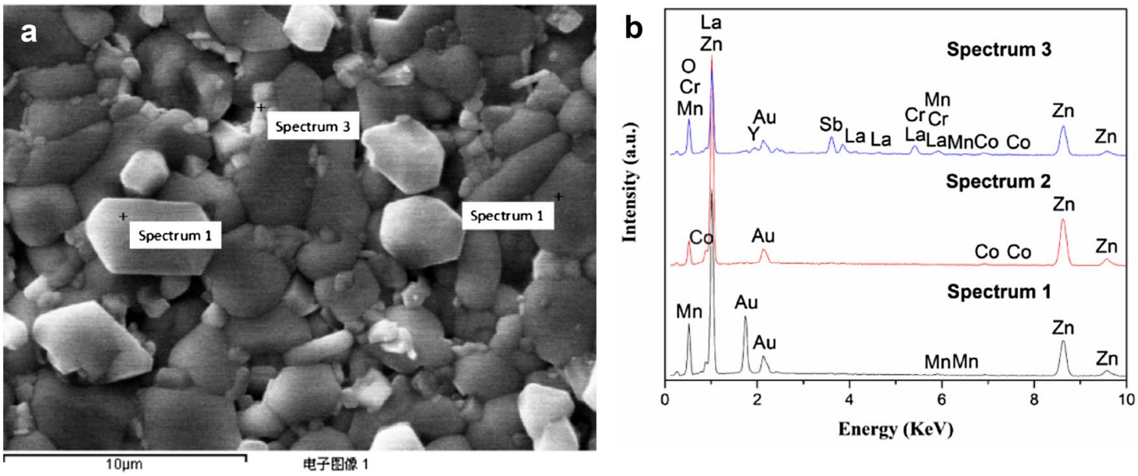

Fig. 3 Results from EDS analysis of the varistor ceramics doped with 0.5 mol% Y_2O_3 sintered at 1100 °C for 2 h: **a** micrograph with marked points, **b** the corresponding EDS spectra

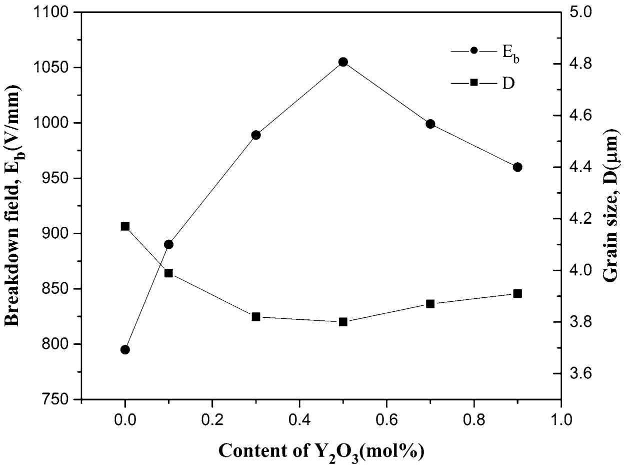

Fig. 4 The variation of breakdown field, E_b, and grain size, D, of the varistor ceramics doped with different Y_2O_3 content sintered at 1100 °C for 2 h

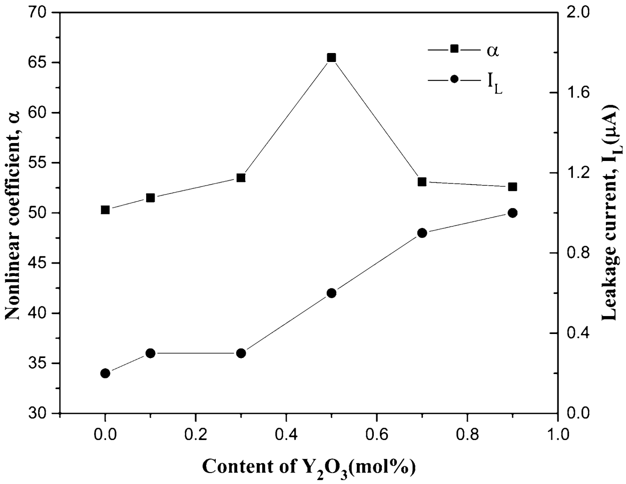

Fig. 5 The variation of the nonlinear coefficient (α) and leakage current (I_L) of ZnO varistor ceramics doped with different Y_2O_3 content sintered at 1100 °C for 2 h

4 Conclusion

The microstructure and electrical properties of Y_2O_3–La_2O_3–Bi_2O_3–ZnO varistor ceramics prepared by a solid-state method from nanosize ZnO powder were investigated. The XRD analyses of the samples evidenced that the microstructure of the ceramics consisted of the ZnO primary phase, spinel phase, Bi_2O_3-rich phase, La-rich phase, Y_2O_3 phase and Y-rich phase. The average grain size of the predominant phases was in the range of 3.80 to 4.17 μm. As Y_2O_3 content increased, the breakdown field E_b initially increased and then decreased. The nonlinear coefficient came to a maximum with 0.5 mol% Y_2O_3 and then descended. The values of leakage current were always below 1.0 μA. Further, the results also showed that varistor ceramics containing 0.5 mol% Y_2O_3 sintered at 1100 °C exhibited comparatively ideal comprehensive electrical properties. (E_b = 1055 V/mm, $\alpha = 65.5$, and I_L = 0.6 μA). But when the amount of Y_2O_3 was higher, the performance of the varistor ceramics descended. And, it can be observed from XRD analyses that the doping of Y_2O_3 affected the decomposition of the spinel; The amounts of spinel decreased with Y_2O_3 content increasing. The results indicated that appropriate amount of Y_2O_3 and La_2O_3 dopant and the application of nanosize ZnO powder can bring ZnO-Bi_2O_3-based varistor ceramics excellent comprehensive electrical properties.

Acknowledgements The authors are grateful for the Project 2014GZ0090 supported by the Science and Technology Support Program in Sichuan.

References

1. C.W. Nahm, J. Alloys Compd. **578**, 132 (2013)
2. G.H. Chen, J.L. Li, C.L. Yuan, Y. Yang, J. Mater. Sci. **24**, 3675 (2013)
3. T.K. Gupta, J. Am. Ceram. Soc. **73**, 1817 (1990)
4. C.W. Nahm, J. Eur. Ceram. Soc **21**, 545 (2001)
5. H.R. Bai, S.H. Li, Y.H. Zhao, Z.J. Xu, R.Q. Chu, J.G. Hao, C. Chen, H.Y. Li, Y.Y. Gong, G.R. Li, Ceram. Int. **42**, 10547 (2016)
6. D.R. Clarke, J. Am. Ceram. Soc. **82**, 485 (1999)
7. S.C. Pillai, J.M. Kelly, R. Ramesh, D.E. McCormack, J. Mater. Chem. C **1**, 3268 (2013)
8. M.A. Ashraf, A.H. Bhuiyan, M.A. Hakim, M.T. Hossain, Mater. Sci. Eng. B **176**, 855 (2011)
9. L.T. Mei, H.I. Hsiang, C.S. Hsi, F.S. Yen, J. Alloys Compd. **588**, 84 (2013)
10. C.W. Nahm, J. Rare Earth **30**, 1028 (2012)
11. Y.J. Dong, F.D. Cui, L. Jiao, H.X. Xu, M. Tang, J.T. Wu, R.H. Yu, D. Xu, J. Cent. South Univ. **20**, 2947 (2013)
12. M. Houabes, R. Metz, Ceram. Int **33**, 1191 (2007)
13. S. Bernik, S. Macek, A. Bui, J. Eur. Ceram. Soc. **24**, 1195 (2004)
14. D. Xu, X.N. Cheng, M.S. Wang, L.Y. Shi, Adv. Mater. Res. **79**, 2007 (2009)
15. Y. Tu, Z. Zheng, X. Li, Q. Wang, M. Luo, L.M. Levinson, Am. Ceram. Soc. **96**, 3518 (2013)
16. L. Ke, D.M. Jiang, C.X. Wang, X.M. Ma, Mod. Phys. Lett. B **23**, 3013 (2009)
17. D. Xu, D.M. Tang, Y.H. Lin, L. Jiao, G.P. Zhao, X.N. Cheng, J. Cent. South Univ. **19**, 1497 (2012)
18. M.A. Ramirez, W. Bassi, R. Parra, P.R. Bueno, E. Longo, J.A. Varela, J. Am. Ceram. Soc. **91**, 2402 (2008)
19. C.W. Nahm, Mater. Lett. **58**, 2252 (2004)
20. C. Yang, D.C. Zhu, T. Zeng, L. Jiao, J. Electron. Mater. **44**, 2651 (2015)